Available online at www.sciencedirect.com
SCIENCE DIRECT®
Polyhedron 22 (2003) 3321–3332
POLYHEDRON
www.elsevier.com/locate/poly

Structural and spectral studies on four coordinate copper(II) complexes of 2-benzoylpyridine $N(4)$,$N(4)$-(butane-1,4-diyl)thiosemicarbazone

Anantharam Sreekanth, Maliyeckal R. Prathapachandra Kurup *

Department of Applied Chemistry, Cochin University of Science and Technology, Kochi, Kerala 682022, India

Received 6 May 2003; accepted 28 July 2003

Abstract

Eight new copper(II) complexes of 2-benzoylpyridine $N(4)$,$N(4)$-(butane-1,4-diyl)thiosemicarbazone (HBpypTsc) with general stoichiometry Cu*BpypTsc*X [X = N_3, Cl, NO_3, NCS, ClO_4, Br, SH and CN] were synthesized and characterized by IR and UV–Vis spectroscopies. The terdentate nature of the ligand is inferred from the IR spectra. Spin Hamiltonian parameters of the compounds were calculated from the EPR spectra. The structures of the compounds Cu*BpypTsc*Cl (**2**), Cu*BpypTsc*Br (**6**) and Cu*BpypTsc*SH (**7**) were solved by single crystal X-ray diffraction. Cu*BpypTsc*Cl (**2**) is a centrosymmetric dimer with chloro bridges. The geometry around copper in other two complexes is square planar.

Keywords: Thiosemicarbazone; Copper(II); Electronic spectra; IR spectra; EPR; X-ray crystal structure

1. Introduction

Thiosemicarbazones have emerged as an important class of sulfur donor ligands particularly for transition metal ions in the last few decades. The real impetus towards developing the coordination chemistry of these thiosemicarbazones has been provided by remarkable biological activities observed for these compounds which has since been shown to be related to their metal complexing ability. These compounds present a great variety of biological activity ranging from anti-tumour, fungicide, bactericide, anti-inflammatory and anti-viral activities [1–4]. We have previously examined the chelating behavior of some ONS and NNS donor thiosemicarbazones in several metal complexes with the aim of gaining more information about their nature of coordination and related structural, spectral and biological properties [5–9]. Herein we report the synthesis and spectral studies of eight new copper(II) complexes of 2-benzoylpyridine (4),$N(4)$-(butane-1,4-diyl)thiosemicarbazone (*HBpypTsc*) (Fig. 1). The crystal structures of three compounds viz., Cu*BpypTsc*Cl (**2**), Cu*BpypTsc*Br (**6**) and Cu*BpypTsc*SH (**7**) are discussed.

2. Experimental

All solvents were distilled before use. 2-benzoylpyridine (Fluka) was used as received. The thiosemicarbazone ligand *HBpypTsc* was prepared by adopting a reported procedure [10], by the condensation of 2-benzoylpyridine and pyrolidine-1-thiocarboxylic acid hydrazide (1:1 molar ratio) in methanol. The mixture was refluxed for 5 h and cooled. Deep yellow crystals of the compound *HBpypTsc* (m.p. 186 °C) were filtered and recrystallised from hot methanol.

2.1. Syntheses of the complexes

Complexes **2**, **3**, **5**, **6** and **7** were prepared by the direct reaction of the appropriate copper salts with the ligand. A solution of the ligand *HBpypTsc* (1 mmol) in

* Corresponding author. Tel.: +91-484-575-804; fax: +91-484-577-595.
E-mail addresses: sreekanth@cusat.ac.in (A. Sreekanth), mrp@cusat.ac.in (M.R. Prathapachandra Kurup).

0277-5387/$ - see front matter © 2003 Elsevier Ltd. All rights reserved.
doi:10.1016/j.poly.2003.07.011

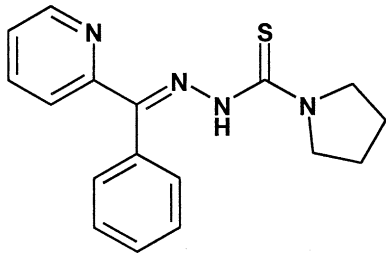

Fig. 1. Structural formulae of the ligand *HBpypTsc*.

chloroform was added to a solution of the appropriate copper salt (1 mmol) in methanol. The deep green colored solution obtained was refluxed for 20 min. The resulting solution yielded shining deep green colored crystals which were filtered and washed with ether and dried over P_4O_{10} in vacuo. The compounds **1**, **4** and **8** were prepared by a metathetical displacement of the acetate anion of the copper acetate complex, by the addition of 1 mmol of NaN_3, KCNS or NaCN in methanol to the reaction mixture of the ligand in chloroform and copper(II) acetate in methanol. The resulting solution was refluxed for 20 min and left overnight. The complexes which separated as tiny crystals were filtered and washed with ether and dried over P_4O_{10} in vacuo. Single crystals suitable for X-ray analysis were grown from a solution of compounds **2**, **6** and **7** in $CHCl_3$ layered with methanol in 5–10 days.

2.2. Physical methods

Micro analyses were carried out using a Heraeus Elemental Analyzer at CDRI, Lucknow, India. Infrared spectra were recorded on a Shimadzu DR 8001 series FT-IR instrument as KBr pellets in the range 400–4000 cm^{-1} and far IR spectra were recorded in the range 50–500 cm^{-1} on a NICOLET MAGNA 550 FT-IR spectrometer using polyethylene pellets at RSIC, IIT, Bombay, India. Electronic spectra were recorded in the 900–250 nm range on a JASCO UV–Vis–NIR Spectrophotometer in $CHCl_3$ solution. Magnetic measurements were made in the polycrystalline state on a simple Gouy balance using $Hg[Co(SCN)_4]$ as calibrant. EPR spectra were recorded in a Varian E-112 X-band EPR Spectrometer using TCNE as a standard at RSIC, IIT, Bombay, India.

2.3. X-ray crystallography

A deep green triclinic crystal of Cu*BpypTsc*Cl (**2**) having approximate dimensions $0.315 \times 0.20 \times 0.10$ mm was sealed in a glass capillary, and intensity data were measured at room temperature (293 K) on an Nonius MACH3 diffractometer equipped with graphite-monochromated Mo Kα ($\lambda = 0.70930$ Å) radiation. Unit cell dimensions were obtained using 25 centered reflections in the θ range 1.87°–24.93°. The intensity data were collected by the ω-scan mode for *hkl* ($-8 \leqslant h \leqslant 8$, $-12 \leqslant k \leqslant 13$, $0 \leqslant l \leqslant 14$) in the triclinic system. The trial structure was obtained by direct methods using SHELXL 97 and refined by full-matrix least squares on F^2 (SHELXS 97) [11,12]. The non-hydrogen atoms were refined with anisotropic thermal parameters. All hydrogen atoms were geometrically fixed and allowed to refine using a riding model. Absorption corrections were employed using ψ-scan ($T_{max} = 1.000$ and $T_{min} = 0.991$). A light green monoclinic crystal of the Cu*BpypTsc*Br (**6**) having approximate dimensions $0.35 \times 0.25 \times 0.15$ mm and a dark green monoclinic crystal of the Cu*BpypTsc*SH (**7**) having approximate dimensions $0.40 \times 0.25 \times 0.25$ mm were analyzed in a similar way. The crystallographic data along with details of structure solution refinements are given in Table 1.

3. Results and discussion

All complexes were found to form readily from the reaction mixture of the appropriate copper(II) salts and the ligand *HBpypTsc* in hot methanol/chloroform. The elemental analysis data (Table 2) suggests the formulation Cu*BpypTsc*X [X = N_3, Cl, NO_3, NCS, ClO_4, Br, SH and CN]. All complexes were non-conductors in $CHCl_3$ indicating the coordination of the anions to the metal center. However the formation of compound **7** was unusual. After synthesis the compound was obtained with an approximate composition $Cu_2(BpypTsc)_2SO_4 \cdot H_2O$ (**7a**), but the X-ray quality single crystals grown from methanol/chloroform yielded a compound with the formula Cu*BpypTsc*SH (**7**). All efforts to repeat the experiment failed and yielded a complex with a composition similar to that of the former (**7a**). IR spectral data of the compound **7a** also suggests the presence of a sulfate group in the compound, but room temperature magnetic moment data which is calculated as ≈1.78 BM points to a mononuclear d^9 copper(II) complex. The possibilities of the formation of such an SH coordinated complex is described in a recent report by Anacona et al. [13] which suggests the formation of an mercapto (SH) coordinated tetrahedral Co(II) complex as a by-product. To our knowledge this is a first structural report of a square planar copper(II) ion containing a mercapto group.

3.1. Electronic spectra

The significant electronic absorption bands in the spectra of the complexes recorded in chloroform are presented in Table 3. The spectrum of *HBpypTsc* and its complexes consist of two broad bands in the regions 40,300 and 29,240 cm^{-1}. These bands remained almost unshifted in the complexes and are due to the $\pi \rightarrow \pi^*$ and $n \rightarrow \pi^*$ transitions of the thiosemicarbazone ligand. A

Table 1
Crystal data and structure refinement parameters for the complexes **2**, **6** and **7**

	Cu*BpypTsc*Cl (**2**)	Cu*BpypTsc*Br (**6**)	Cu*BpypTsc*SH (**7**)
Empirical formula	$C_{34}H_{34}Cl_2Cu_2N_8S_2$	$C_{17}H_{17}BrCuN_4S$	$C_{17}H_{18}CuN_4S_2$
Formula weight, M	816.79	452.86	406.01
Temperature, T (K)	298(2)	293(2)	293(2)
Wavelength (Mo Kα) (Å)	0.70930	0.70930	0.70930
Crystal system	triclinic	monoclinic	monoclinic
Space group	$P1$	$P21/n$	$P21/n$
Unit cell dimensions			
a (Å), α (°)	7.5440(8), 65.924(14)	11.1600(8), 90.000(7)	11.1160(9), 90.000(4)
b (Å), β (°)	11.0990(18), 72.261(12)	8.4050(6), 97.931(7)	8.3010(4), 98.012(6)
c (Å) γ (°)	12.258(2), 76.244(11)	18.534(2), 90.000(6)	18.6780(11), 90.000(5)
Volume, V (Å^3)	884.9(2)	1721.9(3)	1706.67(19)
Z, Calculated density; ρ (Mg m^{-3})	1; 1.533	4; 1.747	4; 1.580
Absorption coefficient, μ (mm^{-1})	1.509	3.716	1.530
$F(000)$	416	908	836
Crystal size (mm)	$0.315 \times 0.20 \times 0.10$	$0.35 \times 0.25 \times 0.15$	$0.40 \times 0.25 \times 0.25$
θ Range for data collection (°)	1.87–24.93	2.01–24.92	2.01–24.93
Limiting indices	$-8 \leqslant h \leqslant 8$, $-12 \leqslant k \leqslant 13$, $0 \leqslant l \leqslant 14$	$0 \leqslant h \leqslant 13$, $0 \leqslant k \leqslant 9$, $-22 \leqslant l \leqslant 21$	$0 \leqslant h \leqslant 13$, $0 \leqslant k \leqslant 9$, $-22 \leqslant l \leqslant 21$
Reflections collected/unique	2889/2889 [$R_{int} = 0.000$]	2763/2763 [$R_{int} = 0.000$]	2844/2844 [$R_{int} = 0.000$]
Completeness to 2θ	24.93°, 88.5%	24.92°, 85.3%	24.93°, 88.0%
Maximum and minimum transmission	1.000 and 0.957	1.000 and 0.980	1.000 and 0.971
Goodness-of-fit on F^2	1.072	1.080	1.087
Final R indices [$I > 2\sigma(I)$]	$R_1 = 0.0392$, $wR_2 = 0.0965$	$R_1 = 0.0275$, $wR_2 = 0.0631$	$R_1 = 0.0276$, $wR_2 = 0.0734$
R indices (all data)	$R_1 = 0.0512$, $wR_2 = 0.1086$	$R_1 = 0.0359$, $wR_2 = 0.0699$	$R_1 = 0.0299$, $wR_2 = 0.0749$
Largest differential peak and hole (e Å^{-3})	0.560 and −0.537	0.578 and −0.346	0.442 and −0.504

Table 2
Colors and partial elemental analysis data of the complexes

Compound	Formula	μ (BM)	Color	Found (Calculated) (%)		
				C	H	N
HBpypTsc	$C_{17}H_{18}N_4S$		deep yellow	65.72 (65.78)	5.81 (5.84)	18.00 (18.05)
Cu*BpypTsc*N_3 (**1**)	$C_{17}H_{17}CuN_7S$	1.82	green	49.86 (49.20)	4.27 (4.13)	23.95 (23.63)
Cu*BpypTsc*Cl (**2**)	$C_{17}H_{17}ClCuN_4S$	1.99	dark green	50.36 (49.99)	4.32 (4.26)	13.80 (13.77)
Cu*BpypTsc*NO_3 (**3**)	$C_{17}H_{17}CuN_5O_3S$	1.92	moss green	46.87 (46.94)	4.02 (3.94)	15.98 (16.10)
Cu*BpypTsc*NCS (**4**)	$C_{18}H_{17}CuN_5S_2$	2.01	olive green	49.98 (50.16)	3.95 (3.98)	16.13 (16.25)
Cu*BpypTsc*ClO_4 (**5**)	$C_{17}H_{17}ClCuN_4O_4S$	2.01	dark green	43.10 (43.22)	3.55 (3.63)	11.10 (11.86)
Cu*BpypTsc*Br (**6**)	$C_{17}H_{17}BrCuN_4S$	1.76	olive green	45.12 (45.09)	3.75 (3.78)	12.24 (12.37)
Cu*BpypTsc*SH (**7**)	$C_{17}H_{18}CuN_4S_2$		dark green	50.24 (50.29)	4.38 (4.45)	13.20 (13.80)
(Cu*BpypTsc*)$_2SO_4 \cdot H_2O$ (**7a**)	$C_{34}H_{36}Cu_2N_8O_5S_3$	1.78	green	46.45 (47.48)	4.02 (4.22)	12.83 (13.03)
Cu*BpypTsc*CN (**8**)	$C_{18}H_{17}CuN_5S$	1.82	dark green	54.22 (54.19)	4.20 (4.29)	17.17 (17.55)

Table 3
Electronic spectral data of the complexes, cm^{-1} (log ε, l mol^{-1} cm^{-1})

Complex	$\pi \rightarrow \pi^*$	$n \rightarrow \pi^*$	LMCT	$d \rightarrow d$
HBpypTsc	40322 (2.69)	36231 (2.54), 29761 (2.25)		
Cu*BpypTsc*N_3 (**1**)	41666 (2.69)	37313 (2.42), 32467 (2.42)	24154 (2.28), 22123 (2.21), 21551 (1.67)	16949 (0.95)
Cu*BpypTsc*Cl (**2**)	41322 (2.64)	37878 (2.52), 31847 (2.57)	26737 (2.25), 22935 (2.57), 22123 (2.56)	16393 (0.96)
Cu*BpypTsc*NO_3 (**3**)	41669 (2.65)	36764 (2.48), 31645 (2.5)	26881 (2.17), 23148(2.25), 22123 (2.56)	16835 (0.84)
Cu*BpypTsc*NCS (**4**)	40983 (2.65)	37313 (2.52), 32467 (2.50)	24390 (2.27), 23041 (2.01), 21834 (2.58)	17301 (0.85)
Cu*BpypTsc*ClO_4 (**5**)	40485 (2.54)	37313 (2.46), 31446 (2.55)	24572 (2.08), 22522 (2.26), 21739(1.98)	16205 (0.92)
Cu*BpypTsc*Br (**6**)	41322 (2.68)	36496 (2.33), 31847 (2.54)	26455 (2.03), 23401 (2.05), 22123 (2.40)	16891 (0.68)
(Cu*BpypTsc*$_2SO_4$ (**7a**))	40322 (2.68)	37314 (2.57), 32051 (2.54)	25906 (2.32), 23148 (2.03), 22026 (2.56)	16611 (0.87)
Cu*BpypTsc*CN (**8**)	40816 (2.71)	37037 (2.41), 31847 (2.32)	26737 (2.17), 23696 (2.13), 21881 (2.45)	16447 (0.92)

second $n \rightarrow \pi^*$ band which is found above at ≈29,000 cm^{-1} in the spectrum of uncomplexed thiosemicarbazone was slightly shifted due to complexation. This is an indication of the enolization followed by the deprotonation of the ligand during complexation. These spectra are consistent with that of square planar species [14]. All complexes exhibit a $d \rightarrow d$ band as weak shoulders in the visible region whose maximum of absorption lie in the

visible region ≈ 16,000 cm^{-1}. Such a feature is expected for a square planar chromophore in accordance with earlier reports [15,16]. For the square planar complexes with $d_{x^2-y^2}$ ground state, three spin allowed transitions are possible viz., $^2B_{1g} \rightarrow {}^2A_{1g}$ ($d_{x^2-y^2} \rightarrow d_{z^2}$), $^2B_{1g} \rightarrow {}^2B_{2g}$ ($d_{x^2-y^2} \rightarrow d_{xy}$) and $^2B_{1g} \rightarrow {}^2E_g$ ($d_{x^2-y^2} \rightarrow d_{xz}, d_{yz}$) and it is difficult to resolve it into three bands. The four lower orbitals are often so close together in energy that individual transfer there from to the upper d level cannot be distinguished and hence the single absorption band. It is observed that the spectra of the complexes are dominated by intense intraligand and charge transfer bands. These intense bands cause the low energy bands to appear as weak shoulders. Metal to ligand CT bands are found at ≈ 26,000–21000 cm^{-1} in the complexes and in accordance with previous studies of copper(II) complexes with similar types of ligands [4,5,7], the higher energy bands are assignable to S → Cu(II) LMCT transition, tailing into the visible region. The pyridyl N(π) → Cu(II) CT transition was observed at ≈23,000 cm^{-1} as a weak shoulder. The CT may occur from the p orbital of coordinated ketonic sulfur or nitrogen to the vacant d orbitals of copper(II). However the coordinated gegenions, X(π) → Cu(II) charge transfer was also observed ≈ 22,000 cm^{-1}.

3.2. Infrared spectra

The significant IR bands with the tentative assignments of the copper(II) complexes in the region 4000–50 cm^{-1} are presented in Table 4. On coordination of the azomethine nitrogen ν(C=N) shifts to lower wavenumbers by 20–50 cm^{-1} [17–19]. The occurrence of ν(NN) at higher wavenumbers in the spectra of the complexes compared to that of the ligand confirm the coordination of the azomethine nitrogen. The IR spectra of the complexes show a new sharp band at ≈ 1630 cm^{-1} which is assigned to the newly formed ν(N=C). This indicates that the ligand enolizes and coordinates in the thiolate form. Coordination via thiolate sulfur is also indicated by the ν/δ(C–S) bands found at ≈ 1294 and 786 cm^{-1}. The ν(Cu–N) stretching frequencies for the azomethine nitrogen are observed around 400 cm^{-1} and the ν(Cu–N) for the pyridyl nitrogen is observed at ≈ 360–340 cm^{-1}. The presence of a new band in the 260–280 cm^{-1}range, which is assignable to ν(Cu–S), is another indication of involvement of sulfur coordination.

Compound **2** showed a sharp ν(Cu–Cl) band at 304 cm^{-1}, along with the presence of a band at 162 cm^{-1} (ν_b) indicates the bridging character in the Cu–Cl bond. A band at 255 cm^{-1} for compound **6** due to ν(Cu–Br) is suggestive for terminally bonded bromine [20]. The ratio of ν(Cu–Br)/ν(Cu–Cl) is 0.83, which is consistent with the usual values obtained for complexes of first row transition metals. Compound **4** has a very strong band at 2076 cm^{-1}, a medium band at 916 cm^{-1} and a weak

Table 4
IR spectral assignments of the complexes

Compound	ν(C=N)	ν(N=C)	ν(N–N)	ρ i.p	ρ o.p	ν (Cu–Npy)	ν (Cu–N_{azo})	ν(X)[#]	ν/δ(C=S)	ν(Cu–S)
HbpypTsc	1630s		1118m	455w	649w				1342s, 842 m	
Cu*BpypTsc*N_3 **(1)**	1544s	1633s	1116m	406w	643w	348m	409m	2044s, 1286m, 575w	1342s, 842m	265w
Cu*BpypTsc*Cl **(2)**	1592s	1634s	1124m	405w	641w	345m	392m	304s, 162s	1334s, 785m	267w
Cu*BpypTsc*NO_3 **(3)**	1575s	1632s	1119m	410w	645w	350m	398m	1493s, 1278s, 1379s, 1010m	1278s, 790m	264w
Cu*BpypTsc*NCS **(4)**	1547s	1633s	1114m	411w	639w	347m	393m	2076s, 916m, 506w	1287s, 786m	262w
Cu*BpypTsc*ClO_4 **(5)**	1540s	1630s	1129m	408w	621w	345m	398m	1156s, 1092s, 908m, 381m	1294s, 783m	280w
Cu*BpypTsc*Br **(6)**	1542s	1628s	1124m	409w	641w	355m	408m	255s	1272s, 783m	279w
(Cu*BpypTsc*)SO_4 **(7a)**	1596s	1635s	1116m	398w	642w	352m	418m	1161s, 905m, 575w	1276s, 785m	280w
Cu*BpypTsc*CN **(8)**	1593s	1634s	1120m	405w	644w	357m	421m	2091s, 467m, 302m, 151m	1268s, 785m	281w

All values are reported in units of cm^{-1}.
[#] X = N_3, Cl, NO_3, NCS, ClO_4, Br, SO_4, CN.

band at 506 cm^{-1} corresponding to ν(CN), ν(CS) and δ(NCS) modes of the NCS group, respectively [21]. The intensity and position of these bands indicate the unidentate coordination of the thiocyanate group through the nitrogen. The ν(Cu–N) is observed at 321 cm^{-1}, which confirms that the N atom of the thiocyanate is coordinated to the metal. We found that compound **3** has four strong bands at 1493, 1379, 1278 and 1010 cm^{-1} corresponding to ν_1, ν_2, ν_4 and ν_5 of the nitrato group indicating the presence of a terminal monodentate coordination of the nitrato group [22]. A combination band $\nu_1 + \nu_4$, considered as diagnostic for the mono coordinate nitrato group, has been observed at 1742 cm^{-1}. ν_3 and ν_6 could not be assigned due to the richness of the spectra of the complex. The ν(Cu–N) of the N-nitrato compound is found at 309 cm^{-1}. Compound **5** showed single broad bands at 1156, and 1092, and a strong band at 621 and a weak band at 908 cm^{-1} indicating the presence of coordinated perchlorate [23]. The coordination is confirmed by a ν(Cu–O) band at 385 cm^{-1}. The band at 1156 cm^{-1} is assignable to $\nu_3(ClO_4)$ and the band at 621 cm^{-1} assignable to $\nu_4(ClO_4)$. The azido complex (**1**) shows a single broad band at 2044 cm^{-1} and a strong band at 1286 cm^{-1}. These are assigned to ν_a and ν_s of the coordinated azido group. The broad bands observed at 575 and 446 cm^{-1} are assigned to δ(N–N–N) and ν(Cu–N) vibrations. This suggests that the Cu–N–N–N bond is linear. Compound **8** showed a sharp absorption near 2091 cm^{-1} indicating the ν(CN) vibration. Coordination of Cu–CN is confirmed by the bands at 450 cm^{-1} ν(Cu–C), 450 cm^{-1} δ(Cu–C–N), and 151 cm^{-1} δ(NC–Cu–S). All complexes showed the in-plane and out-of-plane ligand vibrations (ρ) of the pyridyl ring moiety approximately at ≈400 and 640 cm^{-1}, respectively.

3.3. Electron paramagnetic resonance spectra

The EPR spectra of a polycrystalline sample at 298 K, solution at 298 and 77 K were recorded in the X band, using 100-kHz field modulation; g factors were quoted relative to the standard marker TCNE ($g = 2.0277$). The EPR parameters of the copper(II) complexes are presented in Table 5. The copper(II) ion, with a d^9 configuration, has an effective spin of $S = 3/2$ and is associated with a spin angular momentum $m_s = \pm 1/2$, leading to a doubly degenerate spin state in the absence of a magnetic field. In a magnetic field this degeneracy is lifted and the energy difference between these states is given by $E = h\nu = g\beta H$ where h is the Planck's constant, ν is the frequency, g is the Landé splitting factor (equal to 2.0023 for a free electron), β is the electronic Bohr magneton and H is the magnetic field. For the case of a $3d^9$ copper(II) ion the appropriate spin Hamiltonian assuming a B_{1g} ground state is given by [31]

$$H = \beta[g_{\parallel} H_z S_z + g_{\perp}(H_x S_x + H_y S_y)] + A I_z S_z + B(I_x S_x + I_y S_y).$$

The EPR spectra of compounds **3** and **6** in the polycrystalline state (298 K) show only one broad signal at $g \approx 2.09$ (Fig. 2). Such isotropic spectra, consisting of a broad signal and hence only one g-value, arise from extensive exchange coupling through misalignment of the local molecular axes between different molecules in the unit cell (dipolar broadening) and enhanced spin lattice relaxation. This type of spectra unfortunately gives no information on the electronic ground state of the Cu(II) ion present in the complexes. However the spectra of compounds **1**, **2**, **4**, **5**, **7** and **8** show typical axial spectra (Fig. 2) with a well defined $g_{\parallel}$ feature and $g_{\perp}$ feature at values ≈ 2.22 and 2.09. The variation in the $g_{\parallel}$ and $g_{\perp}$ values indicate that the geometry of the compounds in the solid state is affected by the nature of the coordinating gegenions. The geometric parameter G, which is a measure of the exchange interaction between copper centers in the polycrystalline compound, is calculated using the equation

$$G = \frac{(g_{\parallel} - 2)}{(g_{\perp} - 2)}. \quad (1)$$

If $G > 4$, exchange interaction is negligible and if it is less than 4, considerable exchange interaction is indicated in the solid complex. The geometric parameter G for the complexes is found to be in the range 2.1–3.8 indicating that the g values obtained in the polycrystalline samples are near to the molecular g values which indicate the fact that the unit cell of the compounds contains magnetically equivalent sites [24–26]. All complexes with $g_{\parallel} > g_{\perp} > 2$ and a G value falling within this range are consistent with a $d_{x^2-y^2}$ ground state. Hence we assigned a square planar environment in all the complexes.

The solution spectra of all complexes were recorded in $CHCl_3$ at 298 K (Fig. 3). The spectral features of all the complexes clearly show four fairly resolved hyperfine lines (^{65}Cu, $I = 3/2$) corresponding to −3/2, −1/2, 1/2, 3/2 transitions ($\delta = \pm 1$). The signal corresponding to $M_I = -3/2$ splits clearly into five peaks with a superhyperfine (shf) or ligand hyperfine coupling constant A ≈15 G in the spectra of the complexes [27], due to azomethine nitrogen and pyridyl nitrogen atoms. In the case of compound **2** this signal splits into nine shf lines showing the differences between the pyridyl and azomethine nitrogens. The absence of a signal corresponding to ($\Delta Ms = \pm 2$) in the half field rules out the possibility of any Cu–Cu interactions in compound **2**. In the case of compound **8** all signals except that corresponding to $M_I = +3/2$ showed five intense superhyperfine lines with $A \approx 16$ G. These features are characteristic of compounds bound through azomethine nitrogen and an indication that the bonding in solution

Table 5
EPR spectral parameters of the complexes

Compound	State	Temperature (K)	g_{iso}/g_1, g_2	$g_{\parallel}$	$g_{\perp}$	A_{iso}	$A_{\parallel}$	$A_{\perp}$	A_N	G
Cu*BpypTsc*N_3 (**1**)	polycrystalline	298	2.21, 2.08							2.625
	$CHCl_3$	298	2.087							
	$CHCl_3$	77		1.964	1.931		188.25	86.6	15.5	3.038
Cu*BpypTsc*Cl (**2**)	polycrystalline	298	2.20, 2.09							2.166
	$CHCl_3$	298	2.107			110.6			10.25	
	1:1 $CHCl_3$/toluene	77		2.226	2.093		195.2	62.3		2.431
	DMF	77		2.195	2.090					
Cu*BpypTsc*NO_3 (**3**)	polycrystalline	298	2.09							
	$CHCl_3$	298	2.134			112.3			17.51	
	1:1 $CHCl_3$/toluene	77		2.254	2.083					3.175
Cu*BpypTsc*NCS (**4**)	polycrystalline	298	2.26, 2.09							2.841
	$CHCl_3$	298	2.092							
	1:1 CH_3OH/toluene	77		2.228	2.077					2.652
Cu*BpypTsc*ClO_4 (**5**)	polycrystalline	298	2.22, 2.06							3.533
	$CHCl_3$	298	2.147			102.3			17.45	
	1:1 $CHCl_3$/toluene	77		2.229	2.086		169.3	61.6	15.54	2.971
Cu*BpypTsc*Br (**6**)	polycrystalline	298	2.12							
	$CHCl_3$	298	2.102			111.2			16.25	
	1:1 acetone/toluene	77		2.219	2.064		185.5	71.2		3.172
(Cu*BpypTsc*$_2$$SO_4$ (**7**))	polycrystalline	298	2.20, 1.88							
	$CHCl_3$	298	2.099			108.6			15.85	
	1:1 CH_3OH/toluene	77		2.190	2.084		192.5	56.6	17.52	2.375
Cu*BpypTsc*CN (**8**)	polycrystalline	298	2.21, 2.08							3.07
	$CHCl_3$	298	2.097			112.6			15.25	
	1:1 $CHCl_3$/toluene	77		2.206	2.083		193.3	76.7	13.75	2.562
	DMF	77		2.215	2.090					

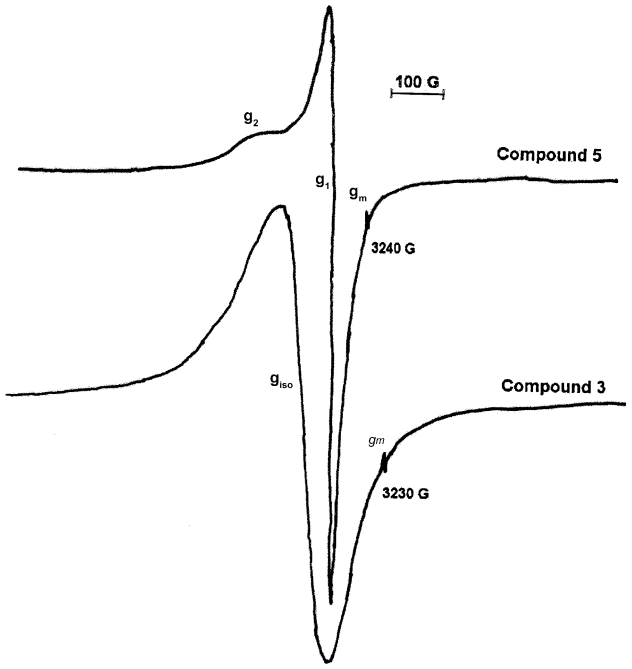

Fig. 2. EPR spectra of compounds **3** and **6** in polycrystalline state at 298 K.

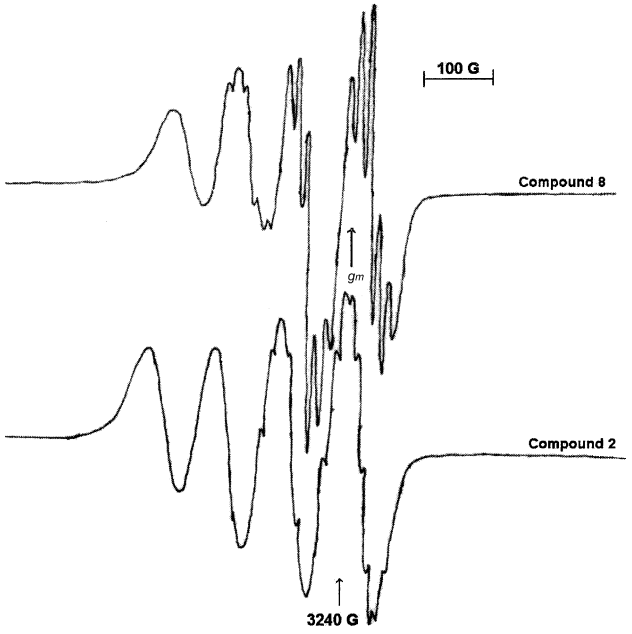

Fig. 3. EPR spectra of compounds **2** and **8** in chloroform at 298 K.

state is dominated by the thiosemicarbazones moiety rather than the mono or polyatomic gegenions.

The EPR spectra of the complexes in glassy state at 77 K was recorded in different solvents like $CHCl_3$, DMF, $CHCl_3$ + toluene (1:1), acetone + toluene (1:1) and methanol + toluene (1:1). However we were unable to get clearly resolved spectra in many cases due to poor glass formation. Some spectra showed three well-resolved peaks of low intensity in the low field region and intense unresolved peaks are obtained in the high field region. The $g_{\|}$, $g_{\perp}$, $A_{\|}$ and $A_{\perp}$ values were calculated accurately from the spectra, while $g_{\perp}$ and $A_{\perp}$ values were confirmed by using the following equations:

$$g_{\perp} = \frac{(3g_{iso} - g_{\|})}{2} \quad \text{and} \quad A_{\perp} = \frac{(3A_{iso} - A_{\|})}{2}. \tag{2}$$

In the parallel region, three of the four copper hyperfine lines are moderately resolved while perpendicular features overlap the fourth one. As is evident from the analysis of the parallel part of the spectra, the line width of the $M_I = -3/2$, component is small compared with the nitrogen coupling constants, leading to the appearance of a nitrogen superhyperfine pattern. The splitting in the perpendicular region of the spectra can be attributed to interaction of an unpaired electron spin with the copper nuclear spin and two ^{14}N ($I = 1$) donor nuclei. The smaller $g_{\|}$ values for the complexes indicated delocalization of the unpaired electron spin density away from the copper nucleus and may be interpreted in terms of increased covalency of the M–L bond [28–30].

There is little difference between the solution spectra obtained at 77 K indicating that the stereochemistry of the complexes is retained on cooling. The $g_{\|} > g_{\perp}$ values suggest a square planar geometry. The $g_{\|}$ values are almost the same for all the compounds, which indicate that the bonding is dominated by the thiosemicarbazones moiety but are different from that in the solid state. Kivelson and Neiman [31] have reported that $g_{\|}$ values less than 2.3 indicate considerable covalent character to M–L bonds and greater than 2.3 indicate ionic character. The $g_{\|}$ values of the complexes are found to be less than 2.3, which indicate considerable covalent character to the M–L bond.

3.4. Molecular and crystal structures of compounds **2**, **6** and **7**

The asymmetric unit of the crystal of compound **2** consists of two molecules characterized by a two-fold axis perpendicular to the Cu1Cl1Cu2Cl2 plane resulting in a centrosymmetric closely associated crystallographically equivalent molecules bridged via chlorine atoms. The comparison of bond distances Cu(2)–Cl(2) (2.253 Å), Cu(2)–Cl(1) (2.776 Å), Cu(1)–Cl(1) (2.253 Å) and Cu(1)–Cl(2) (2.811Å) confirms the possibility of a bridging dinuclear structure, the Cu(1)–Cu(1) distance is also moderate (3.375 Å). These observations agree with the far-IR assignments that the chlorine atoms interact strongly with the metal centre of the neighboring molecule through bridging. This is further confirmed by including the four membered ring Cg(2) = Cu1–C1–Cu2–Cl2 in the analysis of short ring interactions with the program PLATON [1] which indicated that the ring Cg(2) interacts strongly with the

[1] A.L. Spek, PLATON, A multipurpose Crystallographic Tool, University of Utrecht, The Netherlands.

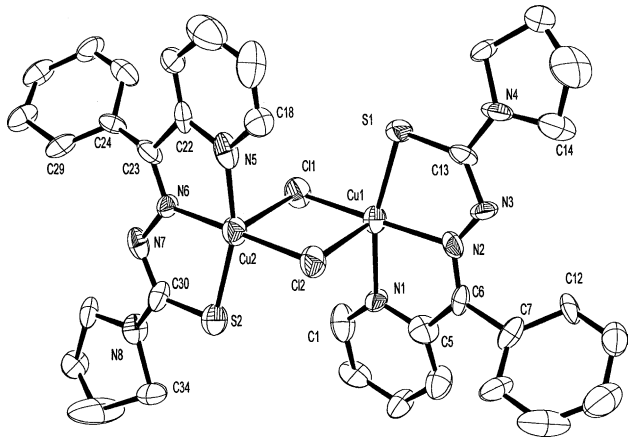

Fig. 4. ORTEP diagram for compound **2** [Cu*BpypTsc*Cl]. Displacement ellipsoids are drawn at the 55% probability level and hydrogen atoms are shown as small spheres of arbitrary radii.

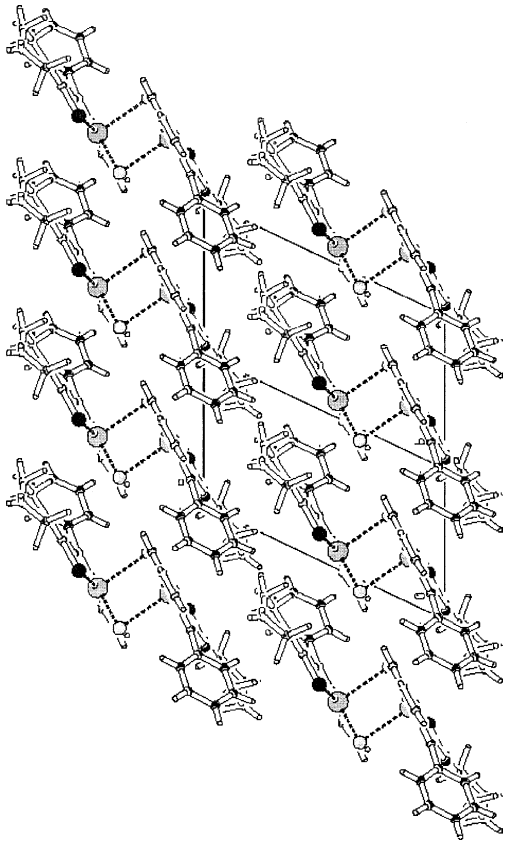

Fig. 5. Packing diagram compound **5** view along *c*-axis.

pyridyl ring of the ligand. The molecular structure along with the atom numbering scheme is presented in Fig. 4, which is found to be square pyramidal around copper. The selected bond lengths and angles are described in Table 6. Coordination lengthens the thiosemicarbazone moiety's C(13)–S(1) bond length from 1.681 to 1.734 Å which is consistent with a C–S single bond length [32–34]. The copper atom is in the same plane with the coordinating Cl(1), azomethine nitrogen N(2), pyridyl nitrogen N(1) and thiolate sulfur S(1) indicated by the bond angles N(1)–Cu(1)–N(2) (82.9°), N(2)–Cu(1)–Cl(1) (174.3°), N(1)–Cu(1)–Cl(1) (95.5°). The bond angles are quite far from a perfect square pyramidal geometry. Similar features are observed for the complexes Cu*BpypTsc*Br (**6**) and Cu*BpypTsc*SH (**7**). The molecular structures of the complexes are shown in Figs. 6 and 8. The Cu–N and Cu–S bond lengths are similar in the three compounds. It is found that the copper atom is closer to the thiosemicarbazone moiety than the gegenions. This is in accordance with the results obtained from EPR spectra.

As Fig. 5 shows, compound **2** packs into an offset fashion with intermolecular π–π stacking interactions between the pyridine rings of both molecules and the

Table 6
Comparison of bond lengths and angles of complexes **2**, **6** and **7**

	Cu*BpypTsc*Cl (**2**)	Cu*BpypTsc*Br (**6**)	Cu*BpypTsc*SH (**7**)
Bond lengths (Å)			
Cu1–N1	2.055 (11)	2.017(3)	2.027(19)
Cu1–N2	2.058 (14)	1.977(3)	1.977(18)
Cu1–S1	2.247(5)	2.2461(9)	2.257(7)
Cu1–X(1)[#]	2.253(5)	2.381(5)	2.247(18)
C6–N2	1.280 (2)	1.301(4)	1.304(3)
N3–N2	1.307 (19)	1.357(4)	1.358(3)
C13–S1	1.734 (17)	1.749(3)	1.751(2)
C13–N3	1.337 (19)	1.339(4)	1.337(3)
Bond angles (°)			
N1–Cu1–N2	82.9(5)	80.61(10)	80.44(7)
N1–Cu1–S1	164.4(4)	165.20(8)	165.01(6)
S1–Cu1–X[#]	96.81(18)	95.83(3)	97.36(7)
N1–Cu1–X[#]	95.5(4)	97.94(7)	96.73(8)
S1–Cu1–N2	83.9 (4)	84.84(8)	84.80(2)
N2–Cu1–X[#]	174.3(4)	169.02(8)	169.81(9)

[#] X = Cl, Br, SH.

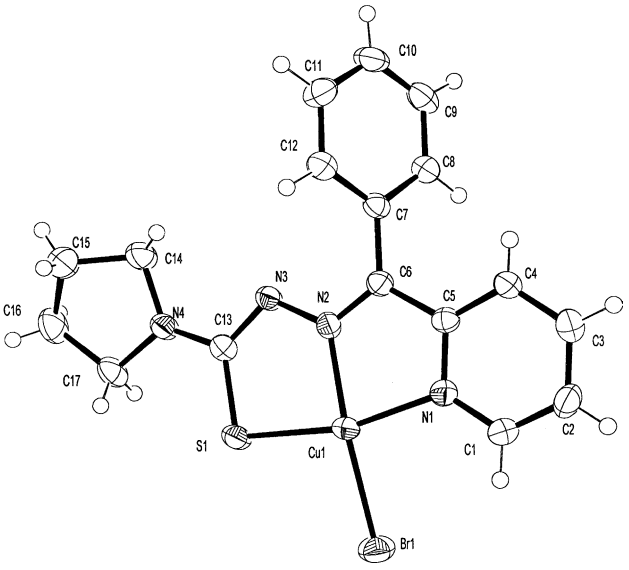

Fig. 6. ORTEP diagram for compound **6** [Cu*BpypTsc*Br]. Displacement ellipsoids are drawn at the 55% probability level and hydrogen atoms are shown as small spheres of arbitrary radii.

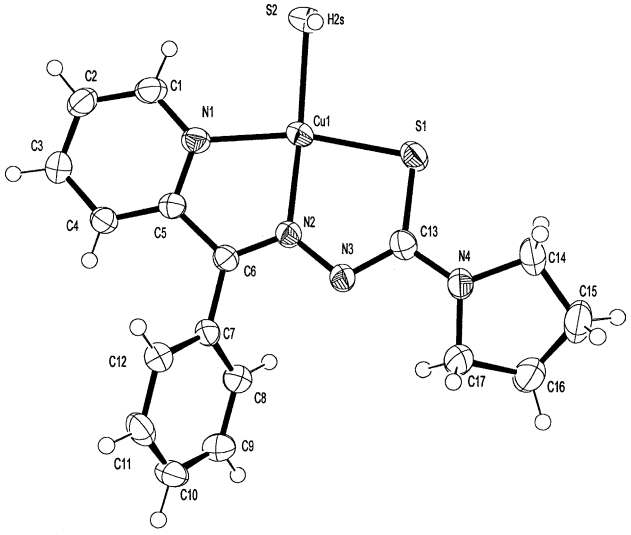

Fig. 8. ORTEP diagram for compound **7** [Cu*BpypTsc*SH]. Displacement ellipsoids are drawn at the 55% probability level and hydrogen atoms are shown as small spheres of arbitrary radii.

four membered ring formed between the two chlorine and copper atoms. The interaction is more related to a π-deficient–π-deficient interaction and will lead to a stable structure [35,36]. The packing is stabilized by the H-bonding and CH...π interactions in the molecule (Table 7). Figs. 7 and 9 show the molecular packing of compounds **6** and **7**. Both molecules pack in a face-to-

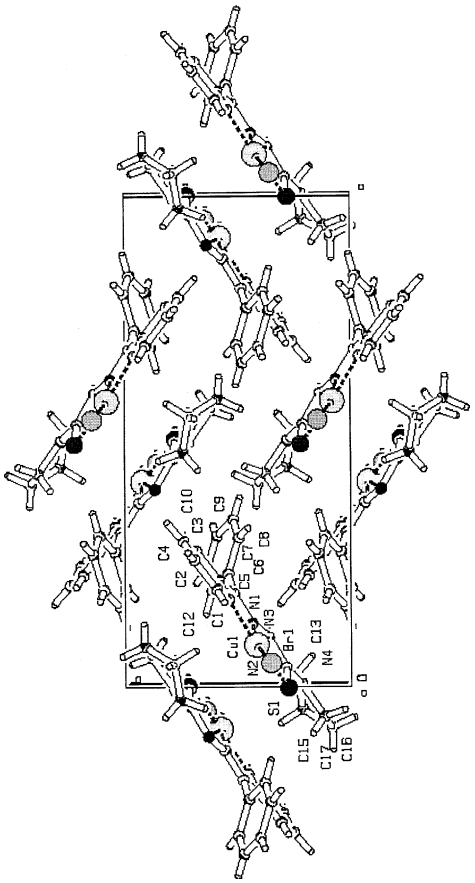

Fig. 7. Packing diagram compound **6** view along *a*-axis.

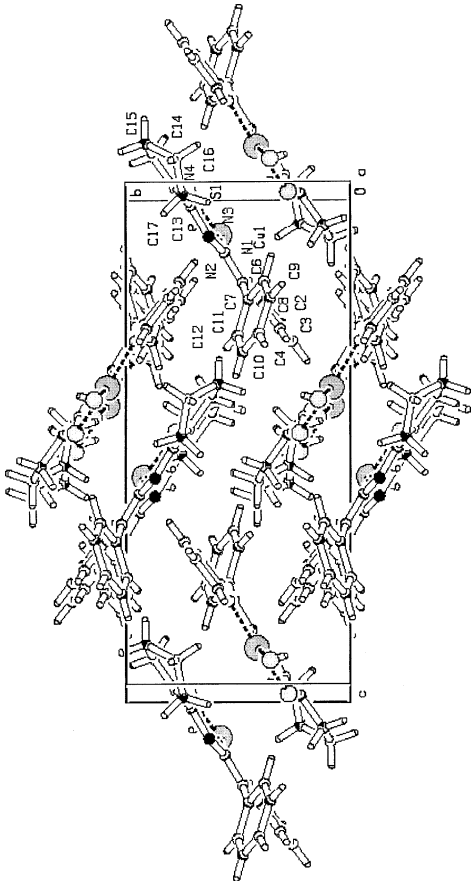

Fig. 9. Packing diagram compound **7** view along *a*-axis.

Table 7
H-bonding, π...π and C–H...π interaction parameters of compound Cu*BpypTsc*Cl (**2**)

D–H···A	D–H (Å)	H···A (Å)	D···A (Å)	∠D–H···A (°)
Intra C(1)–H(1)...Cl(1)	0.93	2.79	3.329	118
C(9)–H(9)...Cl(1)[a]	0.93	2.55	3.697	157
Intra C(12)–H(12)...N(3)	0.93	2.55	2.899	103
C(17)–H(17)...Cl(1)[b]	1.30	2.78	3.949	149
Intra C(18)–H(18)...Cl(2)	0.93	2.76	3.330	120
C(26)–H(26)...Cl(2)[c]	0.93	2.77	3.656	160
Intra C(29)–H(29)...N(7)	0.93	2.53	2.954	108
C(34)–H(34A)...Cl(2)[d]	1.19	2.80	3.886	152
π...π Interactions				
Cg(*I*)–Res(*I*)...Cg(*J*)	Cg–Cg (Å)	α (°)	β (°)	
Cg(2)–[1]...Cg(11)[e]	3.9765	84.15	33.50	
Cg(2)–[1]...Cg(12)[e]	3.9513	87.07	33.28	
CH...π Interactions				
X–H(*I*)----Cg(*J*)	H...Cg (Å)	X...Cg (Å)	∠X–H...Cg (°)	
C(1)–H(1)...Cg(2)[f]	3.0519	3.2714	95.29	
C(3)–H(3)...Cg(13)[g]	2.8591	3.4937	126.54	
C(14)–H(14A)...Cg(11)[h]	2.9284	4.0098	174.56	
C(31)–H(31A)...Cg(12)[g]	2.9393	3.8622	150.23	

Equivalent position code a: $x, 1+y, z$; b: $1+x, y, z$; c: $x, -1+y, z$; d: $-1+x, y, z$; e: x, y, z; f: x, y, x; g: $-1+x, y, z$; h: $1+x, y, z$.
Cg(2) = Cu(1), Cl(1), Cu(2), Cl(2); Cg(11) = N(1), C(1), C(2), C(3), C(4), C(5), C(6); Cg(12) = N(5), C(18), C(19), C(20), C(21), C(22); Cg(13) = C(7), C(8), C(9), C(10), C(11), C(12).
D, donor; A, acceptor; Cg, centroid; α, dihedral angles between planes *I* and *J*; β, angle Cg(*I*) and Cg(*J*).

face manner with an edge-on or T-shaped geometry between the neighboring molecules due to π–σ attraction between the metal containing chelate rings and aromatic hydrogen atoms of the thiosemicarbazone moiety of the molecules. It was interesting to note a ring-metal interaction between the face-to-face packed molecules in compound **7**. The metal chelate ring Cu1–S1–C13–N3–N2 is at a distance of 3.46 Å with the Cu1 of the next molecule. H-bonding and interaction parameters are presented in Tables 8 and 9. Without doubt the most interesting observation is that all three compounds **2**, **6** and **7** exhibit intramolecular stacking parameters which are appropriate enough to consider that effective metal chelate ring/aromatic ring/metal center π...π interactions are operative. To our knowledge these weak intramolecular interactions – π...π, CH...π or chelate ring... metal interactions – involving metal chelate rings can be evidenced for metalloaromaticity – a classic concept recently reviewed by Masui [37]. Interestingly the referred intra- and intermolecular π...π

Table 8
H-bonding, π...π and C–H...π interaction parameters of compound Cu*BpypTsc*Br (**6**)

D–H···A	D–H (Å)	H···A (Å)	D···A (Å)	∠D–H···A (°)
Intra C(1)–H(1)...Br(1)	0.90	2.86	3.4559	124
π...π Interactions				
Cg(*I*)–Res(*I*)...Cg(*J*)	Cg–Cg (Å)	α (°)	β (°)	
Cg(2)–[1]...Cg(2)[a]	3.8238	0.03	37.71	
Cg(2)–[1]...Cg(3)[a]	3.8773	0.67	38.93	
Cg(3)–[1]...Cg(3)[a]	3.9557	0.02	40.23	
Cg(3)–[1]...Cg(8)[b]	3.8910	16.26	19.85	
Cg(4)–[1]...Cg(8)[b]	3.9295	17.80	19.30	
CH...π Interactions				
X–H(*I*)...Cg(*J*)	H...Cg (Å)	X...Cg (Å)	∠X–H...Cg (°)	
C(4)–H(4).....Cg(8)[c]	3.1905	3.4114	98.03	
C(9)–H(9).....Cg(2)[d]	3.1444	3.3379	96.09	

Equivalent position code a: $-x, 1-y, -z$; b: $1/2-x, -1/2+y, 1/2-z$; c: $1/2-x, 1/2+y, 1/2-z$; d: $1/2+x, 1/2-y, -1/2+z$.
Cg(2) = Cu(1), S(1), C(13), N(13); Cg(3) = Cu(1), S(1), C(13), N(3), N(2); Cg(4) = Cu(1), N(1), C(5), C(6), N(2); Cg(8) = C(7), C(8), C(9), C(10), C(11), C(12).
D, donor; A, acceptor; Cg, centroid; α, dihedral angles between planes *I* and *J*; β, angle Cg(*I*) and Cg(*J*).

Table 9
H-bonding, π...π and C–H...π interaction parameters of compound Cu*BpypTsc*SH (**7**)

D–H···A	D–H (Å)	H···A (Å)	D···A (Å)	∠D–H···A (°)
C(1)–H(1)...S(2)	0.90	2.76	3.3465	124
π...π Interactions				
Cg(*I*)–Res(*I*)...Cg(*J*)	Cg–Cg (Å)	α (°)	β (°)	
Cg(2)–[1]...Cg(2)[a]	3.7862	0.02	35.93	
Cg(2)–[1]...Cg(3)[a]	3.8418	0.67	37.28	
Cg(2)–[1]...Cg(8)[b]	3.9977	16.33	24.92	
Cg(3)–[1]...Cg(2)[a]	3.8418	0.67	37.05	
Cg(3)–[1]...Cg(3)[a]	3.9226	0.02	38.71	
Cg(3)–[1]...Cg(8)[b]	3.8833	16.88	19.96	
Cg(4)–[1]...Cg(8)[b]	3.8913	17.90	18.74	
Ring metal interactions				
Cu(1)...Cg(2)[a]	3.336	3.067	23.16	
Cu(1)...Cg(3)[a]	3.460	3.076	27.26	
CH...π interactions				
X–H(*I*)...Cg(*J*)	H...Cg (Å)	X...Cg (Å)	∠X–H–Cg (°)	
C(4)–H(4)...Cg(8)[c]	3.1918	3.3852	96.02	
C(11)–H(11)...Cg(2)[c]	3.1106	3.3185	95.60	
C(11)–H(11)...Cg(3)[c]	3.1896	3.3115	89.98	

Equivalent position code a: $1-x, 1-y, z$; b: $3/2-x, 1/2+y, 1/2-z$; c: $3/2-x, -1/2+y, 1/2-z$.

Cg(2) = Cu(1), S(1), C(13), N(3); Cg(3) = Cu(1), S(1), C(13), N(3), N(2); Cg(4) = Cu(1), N(1), C(5), C(6), N(2); Cg(8) = C(7), C(8), C(9), C(10), C(11), C(12).

D, donor; A, acceptor; Cg, centroid; α, dihedral angles between planes *I* and *J*; β, angle Cg(*I*) and Cg(*J*).

stacking interactions coexist with an extensive 3D hydrogen bonding network.

4. Supplementary information

Crystallographic data for the structural analysis has been deposited with the Cambridge Crystallographic Data Center, CCDC 208631 for compound Cu*BpypTsc*Cl (**2**), CCDC 208632 for compound Cu*BpypTsc*Br (**6**) and CCDC 208633 for compound Cu*BpypTsc*SH (**7**). Copies of this information may be obtained free of charge from The Director, CCDC, 12 Union Road, Cambridge, CB2 IEZ, UK (fax: +44-1223-336-033; e-mail: deposit@ccdc.cam.ac.uk or http://www.ccdc.cam.ac.uk).

Acknowledgements

The authors are thankful to the National Single Crystal X-ray Diffraction Facility, IIT, Bombay for the X-ray diffraction studies, CDRI, Lucknow for elemental analysis and IR spectra, and RSIC, IIT, Bombay for EPR and far-IR data. One of the authors (A.S.) is thankful to Mr. Binoy Paul, International School of Photonics, Cochin University of Science and Technology, Kochi, India for the electronic spectral measurements.

References

[1] J.P. Scovill, D.L. Klayman, C.F. Franchino, J. Med. Chem. 25 (1982) 1261.
[2] M.E. Hossain, M.N. Alam, J. Begum, M.A. Ali, M. Nazimuddin, F.E. Smith, R.C. Hynes, Inorg. Chim. Acta 249 (1996) 207.
[3] P. Bindu, M.R.P. Kurup, T.R. Satyakeerthy, Polyhedron 18 (1999) 321.
[4] M.A. Ali, D.A. Chowdhary, M. Nazimuddin, Polyhedron 3 (1984) 595.
[5] B.S. Garg, M.R.P. Kurup, S.K. Jain, Y.K. Bhoon, Transition Met. Chem. 13 (1988) 309.
[6] R.P. John, A. Sreekanth, M.R.P. Kurup, S.M. Mobin, Polyhedron 21 (2002) 2515.
[7] R.P. John, A. Sreekanth, M.R.P. Kurup, A. Usman, I.A. Razak, H.K. Fun, Spectrochim. Acta 59 A (2003) 1349.
[8] A. Usman, I.A. Razak, S. Chantrapromma, H.K. Fun, A. Sreekanth, S. Sivakumar, M.R.P. Kurup, Acta Crystallogr., Sect. C 58 (2002) m461.
[9] R.P. John, M.R.P. Kurup, National Symposium on Magnetic Resonance and Biomolecular Structure and Function, TIFR, Mumbai, India, January 17–20, 2000, p. L46.
[10] J.P. Scovill, Phosphorous Sulfur Silicon 60 (1991) 25.
[11] G.M. Sheldrick, Shelxl 97, Program for the Solution of Crystal Structures, University of Göttingen, Göttingen, Germany, 1997.
[12] G.M. Sheldrick, Shelxs 97, Program for the Solution of Crystal Structures, University of Göttingen, Göttingen, Germany, 1997.
[13] J.R. Anacona, A. Azocar, O. Nusetti, C.R. Barbarin, Transition Met. Chem. 28 (2003) 24.
[14] A.B.P. Lever, Inorganic Electronic Spectroscopy, 2nd ed., Elsevier, Amsterdam, 1984.
[15] B. Harikumar, M.R.P. Kurup, T.N. Jayaprakash, Transition Met. Chem. 22 (1997) 507.
[16] P. Bindu, M.R.P. Kurup, Transition Met. Chem. 22 (1997) 578.
[17] M.J.M. Campbell, Coord. Chem. Rev. 15 (1975) 279.

[18] B.S. Garg, M.R.P. Kurup, S.K. Jain, Y.K. Bhoon, Transition Met. Chem. 13 (1988) 92.
[19] B.S. Garg, M.R.P. Kurup, S.K. Jain, Y.K. Bhoon, Transition Met. Chem. 13 (1988) 247.
[20] K. Nakamoto, Infrared and Raman Spectra of Inorganic and Coordination Compounds, 5th ed., Wiley, NewYork, 1997.
[21] R.A. Bailey, S.L. Kozak, T.W. Michelsen, W.N. Mills, Coord. Chem. Rev. 6 (1971) 407.
[22] A.B.P. Lever, E. Mantovani, B.S. Ramaswami, Can. J. Chem. 49 (1971) 1957.
[23] B.J. Hathaway, A.E. Underchill, J. Chem. Soc. (1961) 3091.
[24] I.M. Proctor, B.J. Hathaway, P. Nicholis, J. Chem. Soc., A (1968) 1678.
[25] S.K. Jain, B.S. Garg, Y.K. Bhoon, Spectrochim. Acta 42A (1986) 959.
[26] B.J. Hathaway, D.E. Billing, Coord. Chem. Rev. 5 (1970) 1949.
[27] J. Casabo, M. Izaquierdo, J. Ribas, C. Diaz, Transition Met. Chem. 8 (1983) 110.
[28] B.J. Hathaway, in: G. Wilkinson, R.D. Gillard, J.A. McCleverty (Eds.), Comprehensive Coordination Chemistry II, vol. 5, Pergamon, Oxford, 1987, p. 533.
[29] A.H. Maki, B.R. McGravey, J. Chem. Phys. 28 (1958) 35.
[30] V.H. Growford, W.E. Hatfield, Inorg. Chem 16 (1977) 1336.
[31] D. Kivelson, R. Neiman, J. Chem. Phys. 35 (1961) 149.
[32] A. Sreekanth, M.R.P. Kurup, unpublished results.
[33] A. Sreekanth, S. Sivakumar, M.R.P. Kurup, J. Mol. Struct. 655 (2003) 47.
[34] A. Usman, I.A. Razak, S. Chantrapromma, H.K. Fun, V. Philip, A. Sreekanth, M.R.P. Kurup, Acta Crystallogr., C 58 (2002) o652.
[35] C. Janiak, J. Chem. Soc., Dalton. Trans. (2000) 3885.
[36] B.H. Ye, X.M. Chen, G.Q. Xue, L.N. Ji, J. Chem. Soc., Dalton Trans. (1998) 2827.
[37] H. Masui, Coord. Chem. Rev. 219–221 (2001) 957.